Developmental Cell
Article

Anterograde Transport of TrkB in Axons Is Mediated by Direct Interaction with Slp1 and Rab27

Nariko Arimura,[1] Toshihide Kimura,[1] Shinichi Nakamuta,[1] Shinichiro Taya,[1,2] Yasuhiro Funahashi,[1,2] Atsushi Hattori,[1] Akiko Shimada,[1] Céline Ménager,[1] Saeko Kawabata,[1] Kayo Fujii,[1] Akihiro Iwamatsu,[3] Rosalind A. Segal,[4] Mitsunori Fukuda,[5] and Kozo Kaibuchi[1,2,*]

[1]Department of Cell Pharmacology, Graduate School of Medicine, Nagoya University, 65, Tsurumai, Showa, Nagoya, 466-8550, Japan
[2]JST, CREST, 4-1-8, Honcho, Kawaguchi, 332-0012, Japan
[3]Central Laboratories for Key Technology, Kirin Brewery Co. Ltd., 1-13-5 Fukuura, Kanazawa, Yokohama, 236-0004, Japan
[4]Department of Neurobiology, Harvard Medical School and Department of Pediatric Oncology, Dana-Farber Cancer Institute, 44 Binney Street, Boston, MA 02115, USA
[5]Laboratory of Membrane Trafficking Mechanisms, Department of Developmental Biology and Neurosciences, Graduate School of Life Sciences, Tohoku University, Aobayama, Aoba, Sendai, 980-8578, Japan
*Correspondence: kaibuchi@med.nagoya-u.ac.jp
DOI 10.1016/j.devcel.2009.03.005

SUMMARY

The neurotrophin receptors TrkA, TrkB, and TrkC are localized at the surface of the axon terminus and transmit key signals from brain-derived neurotrophic factor (BDNF) for diverse effects on neuronal survival, differentiation, and axon formation. Trk receptors are sorted into axons via the anterograde transport of vesicles and are then inserted into axonal plasma membranes. However, the transport mechanism remains largely unknown. Here, we show that the Slp1/Rab27B/CRMP-2 complex directly links TrkB to Kinesin-1, and that this association is required for the anterograde transport of TrkB-containing vesicles. The cytoplasmic tail of TrkB binds to Slp1 in a Rab27B-dependent manner, and CRMP-2 connects Slp1 to Kinesin-1. Knockdown of these molecules by siRNA reduces the anterograde transport and membrane targeting of TrkB, thereby inhibiting BDNF-induced ERK1/2 phosphorylation in axons. Our data reveal a molecular mechanism for the selective anterograde transport of TrkB in axons and show how the transport is coupled to BDNF signaling.

INTRODUCTION

During neuronal development, neurons develop two types of neurites, axons and dendrites, as they establish polarity. Axons contain synaptic vesicles, from which they release neurotransmitters at axon termini in response to electrical signals, whereas dendrites contain receptors for the neurotransmitters and synapse at the dendritic spines. Axons and dendrites are structurally and functionally distinct, and their unique features are developed and maintained by the highly specific transport of vesicles and molecules, as well as by localized signaling events (Arimura and Kaibuchi, 2007; Segal, 2003).

Some of the most important regulators for axon formation of hippocampal neurons are neurotrophins and their receptors, TrkA, TrkB, and TrkC (Segal, 2003; Kim et al., 2006). To date, several groups, including ours, have reported that the neurotrophins NT-3 and brain-derived neurotrophic factor (BDNF) accelerate axon formation in cultured rat hippocampal neurons (Yoshimura et al., 2005; Zhou and Snider, 2005). TrkA is activated at the tip of a single neurite preceding axon specification, and it plays a critical role in determining axonal fate (Da Silva et al., 2005). Shelly et al. (2007) have recently shown that localized application of BDNF to an immature neurite induces axon differentiation and elongation. Thus, TrkA localization to the distal part of an axon appears to play an important role in axon formation.

Trk receptors are produced at the cell body, sorted into an axonal shaft via the anterograde transport of the Trk-containing exocytic vesicles along microtubules, and then inserted into the axonal plasma membranes (Segal, 2003). Neurotrophins activate Trks located on axon termini and initiate the signals that culminate in axon outgrowth and neuronal survival. The Trk signal activates Ras, PI3 kinase, and Akt, thereby inactivating glycogen synthease kinase-3β (GSK-3β) to promote axon elongation (Arimura and Kaibuchi, 2007; Segal, 2003). Activated Trks are autophosphorylated and consequently endocytosed at the axonal terminus. Then, the Trk-containing endocytotic vesicles are retrogradely transported toward the cell body by the microtubule-dependent, minus-end-directed motor protein, cytoplasmic dynein (Deinhardt et al., 2006; Gomes et al., 2006). This retrograde transport is necessary for Trk signaling to exert a variety of neuronal functions (Glebova and Ginty, 2005; Segal, 2003).

Anterograde transport of the vesicles and molecules including Trk is mediated mainly by microtubule-dependent, plus-end-directed motor proteins, i.e., kinesins (Goldstein, 2001; Hirokawa and Takemura, 2005). Kinesin-1, a conventional member of the kinesin family, is a tetramer of two kinesin heavy chains (KIF5A, KIF5B, or KIF5C) and two kinesin light chains (KLC1 or KLC2). Kinesin-1 associates with the cargoes, including the receptors and adhesion molecules on the vesicles, through specific cargo receptors such as JIPs (Verhey et al., 2001), and it specifically transports the cargo-containing vesicles into axons and dendrites. There are only a few known cargo receptors, most of which are poorly characterized, and they cannot account for the selective transport of vesicles containing different cargoes.

Moreover, it remains largely unknown how a variety of cargoes are recognized by the specific cargo receptors and how their interactions are spatially and temporally regulated.

We previously found that collapsin response mediator protein-2 (CRMP-2), also known as TOAD-64, Ulip2, and DRP-2, is crucial for axon formation in hippocampal neurons (Fukata et al., 2002; Inagaki et al., 2001; Nishimura et al., 2003). Overexpression of CRMP-2 induces the formation of multiple axons, and inhibition of CRMP-2 function prevents axon formation (Inagaki et al., 2001). We have recently found that CRMP-2 interacts with KLC and accumulates in the distal part of growing axons in a manner dependent on Kinesin-1 (Kimura et al., 2005). CRMP-2 links Kinesin-1 to specific proteins such as tubulin heterodimers and the Sra-1/WAVE complex, thereby promoting their anterograde transport in axons as a cargo receptor (Kawano et al., 2005; Kimura et al., 2005; Tsuboi et al., 2005). In addition, CRMP-2 seems to localize to vesicular structures in axonal growth cones, although the nature of the vesicles remains to be clarified (Kawano et al., 2005; Takamori et al., 2006). This finding raises the possibility that CRMP-2 participates not only in the transport of soluble molecules such as tubulin and Sra-1/WAVE, but also as a cargo receptor in the transport of specific vesicles.

In light of these observations, we hypothesized that CRMP-2 was involved in the anterograde transport of the vesicles containing Trks. We here report that CRMP-2, Slp1 (also known as JFC1 or Exophilin-7), and Rab27 form a complex; associate with the cytoplasmic region of TrkB in a Rab27-dependent fashion; and regulate the anterograde transport of TrkB through Kinesin-1.

RESULTS

CRMP-2 Forms a Complex with TrkB

To understand the relationship between CRMP-2 and Trks, we first compared the subcellular distribution of CRMP-2 and Trks in cultured hippocampal neurons. We used pan-specific Trks antibody to examine the localization of all isoforms of Trks. Because CRMP-2 forms a cytoplasmic complex with tubulin dimers, under conventional fixation conditions it shows diffuse cytoplasmic staining (Inagaki et al., 2001). However, when we examined the localization of CRMP-2 and Trks by using an extraction method that is useful for removing cytosolic components and visualizing cytoskeleton- or membrane-associated components (Figure 1A) (this method is described in Supplemental Data available online), CRMP-2 colocalized clearly with microtubules (Figure 2E), consistent with its coassembly into microtubules (Fukata et al., 2002) and its formation of a complex with Kinesin-1 (Kimura et al., 2005). Trks are localized at the plasma membrane and in anterograde or retrograde transport vesicles (Deinhardt et al., 2006; Gomes et al., 2006). We found that Trks-containing vesicles are present in the perinuclear region and in the central region of growth cones (Figure 1A). Trks-containing vesicular structures are partially colocalized with CRMP-2 at the neurite shaft and the central region of the growth cones (87.2% ± 3.6% of Trk^+ puncta was $CRMP\text{-}2^+$, n = 3).

Because TrkB is a major receptor for BDNF and is involved in axon formation, we examined whether CRMP-2 forms a complex with TrkB. When CRMP-2 was immunoprecipitated from rat brain lysate, TrkB was coimmunoprecipitated (Figure 1B). Reciprocally, CRMP-2 was coimmunoprecipitated with TrkB (Figure 1B), suggesting that CRMP-2 and TrkB form a complex in vivo. We next examined whether CRMP-2 directly binds to TrkB and found that CRMP-2 did not associate with the cytoplasmic region of TrkB in a cell-free system (Figure S1A), suggesting that the association is indirect.

Slp1 Interacts with CRMP-2

To explore the missing link between CRMP-2 and Trks, we searched for novel CRMP-2-binding molecules in rat brain lysates (embryonic day 19 [E19]) by using affinity column chromatography and mass spectrometry, as described previously (Fukata et al., 2002). We identified Slp1, an effector of Rab27, as a CRMP-2-interacting molecule. As Slp1 associates with melanosomes and regulates their transport in melanocytes, it seemed to be a potential candidate for connecting CRMP-2 to vesicles (Kuroda et al., 2002; Strom et al., 2002). CRMP-2 and Slp1 were reciprocally coimmunoprecipitated from rat brain lysate (Figure 1C), suggesting that they form a complex in vivo.

We then examined whether CRMP-2 directly binds to Slp1 and found that His-tagged CRMP-2 (His-CRMP-2) bound to GST-fused Slp1 (GST-Slp1), but not to GST or GST-Slp2-b, another member of the Slp family (Figure 1D). The binding of His-CRMP-2 to GST-Slp1 was dose dependent and saturable (Figure 1E). Scatchard analysis revealed a single class of affinity binding sites with a binding dissociation constant (K_D) of ~0.1 ± 0.05 μM.

We also identified the interacting regions of CRMP-2 and Slp1 by using an in vitro binding assay with purified deletion constructs. Slp1 has a Rab27-binding domain at the N terminus and a tandem C2 domain (C2AB) at the C terminus (Figure 1F) (Fukuda and Mikoshiba, 2001; Izumi et al., 2003). CRMP-2 bound strongly to the N-terminal Slp1 homology domain (amino acids [aa] 1–109) and weakly to the C2AB domain (aa 268–567) of Slp1 (Figure 1F). Slp1 bound to aa 348–572 and aa 382–440 of CRMP-2 (Figure 1G). These results indicate that CRMP-2 (aa 382–440) directly binds to the N-terminal domain of Slp1 (aa 1–109).

As the CRMP-2-binding region (aa 1–109) of Slp1 contains the Rab27-binding site (aa 32–72) (Fukuda, 2002), we examined which region of Slp1 associates with CRMP-2 in more detail (Figure 1H). The Rab27 subfamily consists of Rab27A and Rab27B. We focused on Rab27B because it is strongly expressed in the brain, whereas Rab27A is weakly expressed (Zhao et al., 2002). An in vitro binding assay revealed that CRMP-2 associates with aa 1–109 and aa 1–40 fragments of Slp1, but not with other regions (Figure 1H), indicating that the aa 1–31 region contains the CRMP-2-binding site. These results indicate that Rab27B and CRMP-2 associate with Slp1 via distinct regions.

Slp1, Rab27, and CRMP-2 Form a Complex

Next, we examined whether Slp1 binds to CRMP-2 and Rab27 simultaneously. Wild-type Flag-tagged Rab27B (Flag-Rab27B WT) plus constitutively active (Q78L) and inactive (T23N) forms were transfected into COS-7 cells together with T7-tagged Slp1 (T7-Slp1) and EGFP-tagged CRMP-2 (EGFP-CRMP-2). When EGFP-CRMP-2 was immunoprecipitated, T7-Slp1 was coimmunoprecipitated in the presence or absence of Flag-Rab27B (Figure 2A). Flag-Rab27B WT and Q78L, but not T23N, were coimmunoprecipitated in the presence of Slp1 (Figure 2A). Similar results were obtained with the use of Rab27A (Figure 2B). GTPγS-bound MBP-Rab27B consistently formed a complex with His-Slp1 and

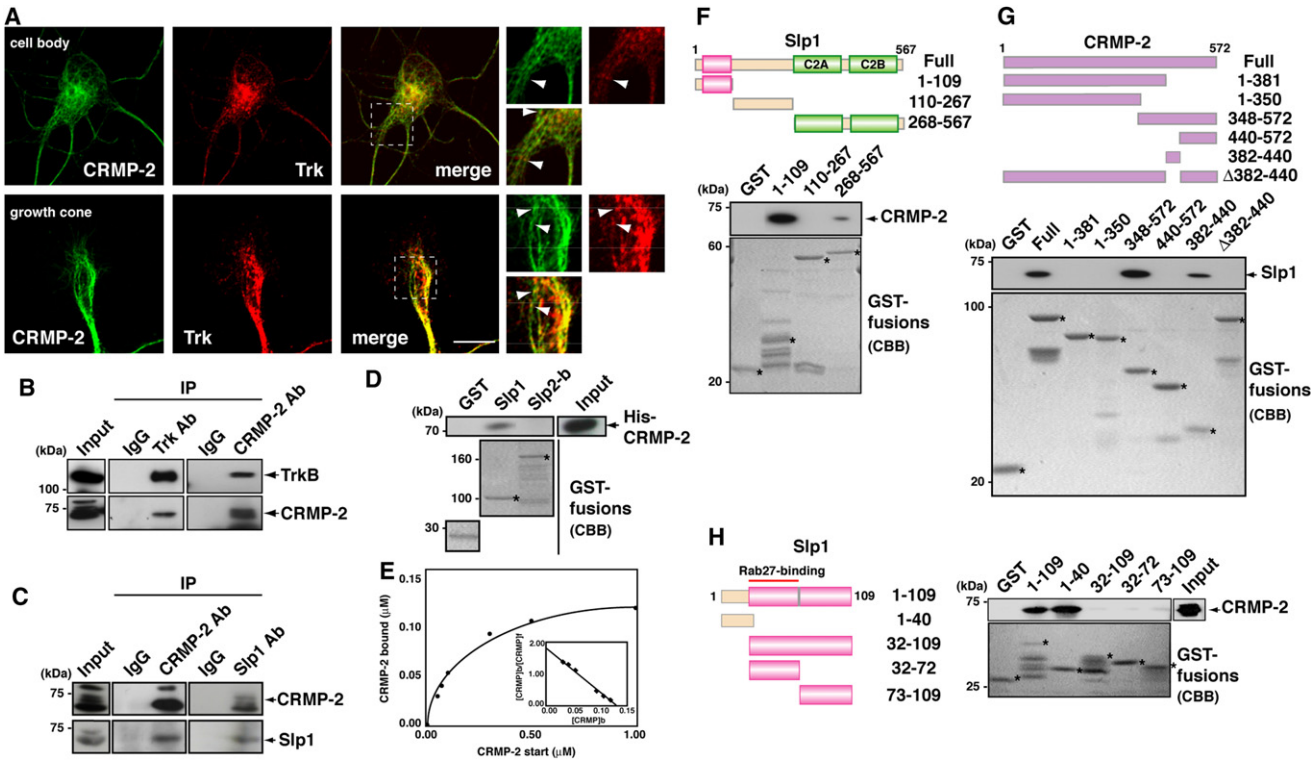

Figure 1. Detection of Slp1 as a Candidate for a Mediator between CRMP-2 and Trk

(A) Colocalization of CRMP-2 and Trk at cell body and growth cone in hippocampal neurons. Pan-specific Trk antibody was used. The scale represents 10 μm.

(B and C) Complex formation of Trk and CRMP-2 in vivo. The input (left; 5%) and immunoprecipitates (IP; right) were analyzed by immunoblotting with the indicated antibodies.

(D) Direct interaction of CRMP-2 with Slp1. GST-fused proteins are indicated by Coomassie brilliant blue (CBB) staining. Asterisks indicate each intact band.

(E) Quantitative analysis of the binding between CRMP-2 and Slp1. The figure represents three experiments that yielded similar binding.

(F) Mapping of the region in Slp1 required for binding to CRMP-2. The domain structure and deletion constructs of Slp1 are shown on the top. The pink box at the N terminus indicates the Slp homology domain containing the Rab27-binding domain, and the green boxes at the C terminus indicate the tandem C2 domain. Numbers refer to amino acid positions.

(G) Mapping of the region in CRMP-2 required for binding to Slp1.

(H) Mapping of the region in Slp1 required for binding to CRMP-2. The Rab27-binding domain (aa 32–72) is indicated by the red bar.

CRMP-2-GST with ~0.2:0.3:1 stoichiometry, whereas GDP-bound Rab27B did not form a complex (Figure 2C). These results suggest that Slp1, GTP-bound Rab27, and CRMP-2 form a complex.

Slp1/Rab27 Localizes on Microtubules with CRMP-2

We compared the subcellular distribution of Slp1, Rab27, and CRMP-2 in cultured hippocampal neurons. Slp1 accumulated at the cell body and the tips of axons in developing neurons (Figure 2D). We further compared the localization of Slp1, Rab27, and CRMP-2 at higher views of axonal growth cones. CRMP-2 was distributed along microtubules at the central region of the growth cones (Figures 2E and 2I). Slp1 localized to vesicular structures that also aligned along microtubules (Figures 2F and 2I), and it was colocalized with Rab27 (Figures 2G and 2I) and partially with CRMP-2 (Figures 2H and 2I) at the central region of the growth cones.

Slp1/Rab27B Associates with TrkB

Next, we compared the localization of Slp1 and Rab27 with Trks and found that Slp1 and Rab27 were partially colocalized with Trks (Figure 3A, data not shown). Slp1 was partially colocalized with Trks, but rarely with phosphorylated Trk proteins (Figure S1B).

We then examined by immunoprecipitation whether TrkB forms a complex with Slp1/Rab27/CRMP-2. When TrkB was immunoprecipitated from rat brain lysates, Slp1 and Rab27 were coimmunoprecipitated (Figure 3B), suggesting that TrkB forms a complex with Slp1/Rab27/CRMP-2 in the brain. The Trk adaptor protein ARMS/Kidins220; the Kinesin-1 adaptor protein JIP1; and the CRMP-2-interacting molecules Sra-1, WAVE1, and Rab8 also coimmunoprecipitated; however, Alcadein α/calsyntenin 1, Rab4, and Rab5 were not detected (Figures S1C and S1D). These results raise the possibility that TrkB associates with several kinds of cargo receptors, such as ARMS/Kidins220 and JIP1 (see Discussion).

How does TrkB associate with the Slp1/Rab27B complex? We first tested which proteins could associate with TrkB in the absence of the other proteins. T7-Slp1 and Flag-Rab27B were coimmunoprecipitated in the absence of Myc-CRMP-2, but not in the absence of each other (Figure 3D), suggesting that both Slp1 and Rab27B, but not CRMP-2, are necessary for the interaction with TrkB. Myc-CRMP-2 was immunoprecipitated weakly

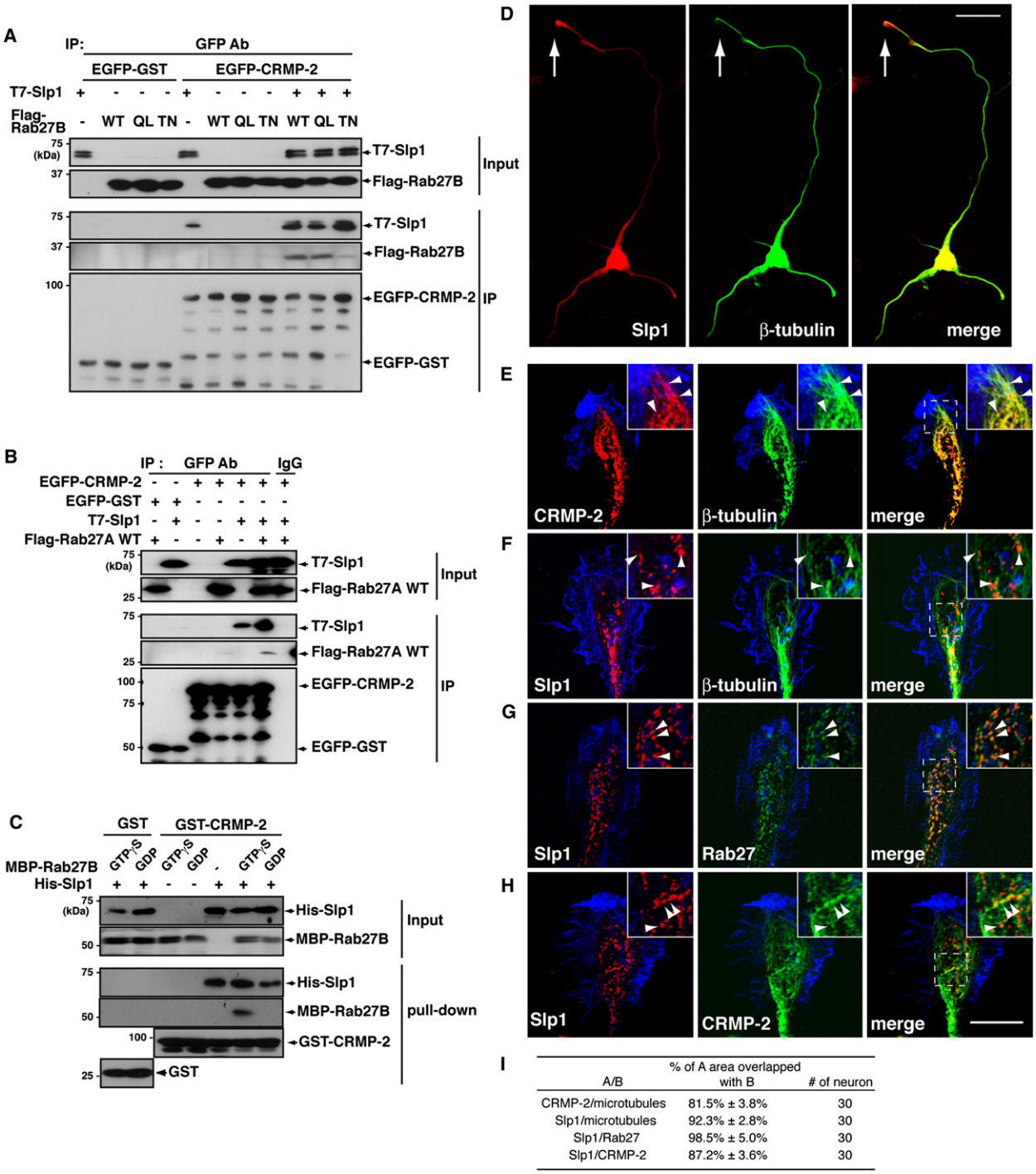

Figure 2. Slp1 Is Colocalized with Rab27, CRMP-2, and Trk

(A) Slp1-dependent association of Rab27B with CRMP-2.

(B) Slp1-dependent association of Rab27A with CRMP-2.

(C) Trimeric complex formation of CRMP-2, Slp1, and the active form of Rab27B in vitro.

(D) Localization of Slp1 in developing hippocampal neurons. Anti-unique type III β-tubulin antibody was used as a neuron marker. Arrows indicate the distal part of the axon. The scale represents 30 μm.

(E–H) Colocalization of CRMP-2, Slp1, and Rab27 on microtubules at growth cones. Arrowheads in the enlarged images indicate colocalization of each protein. The peripheral regions of the growth cones were visualized by staining F-actin with Alexa 647-conjugated phalloidin (blue) in (E)–(H). The scale represents 10 μm.

(I) The percentage of colocalization of each immunolabeling.

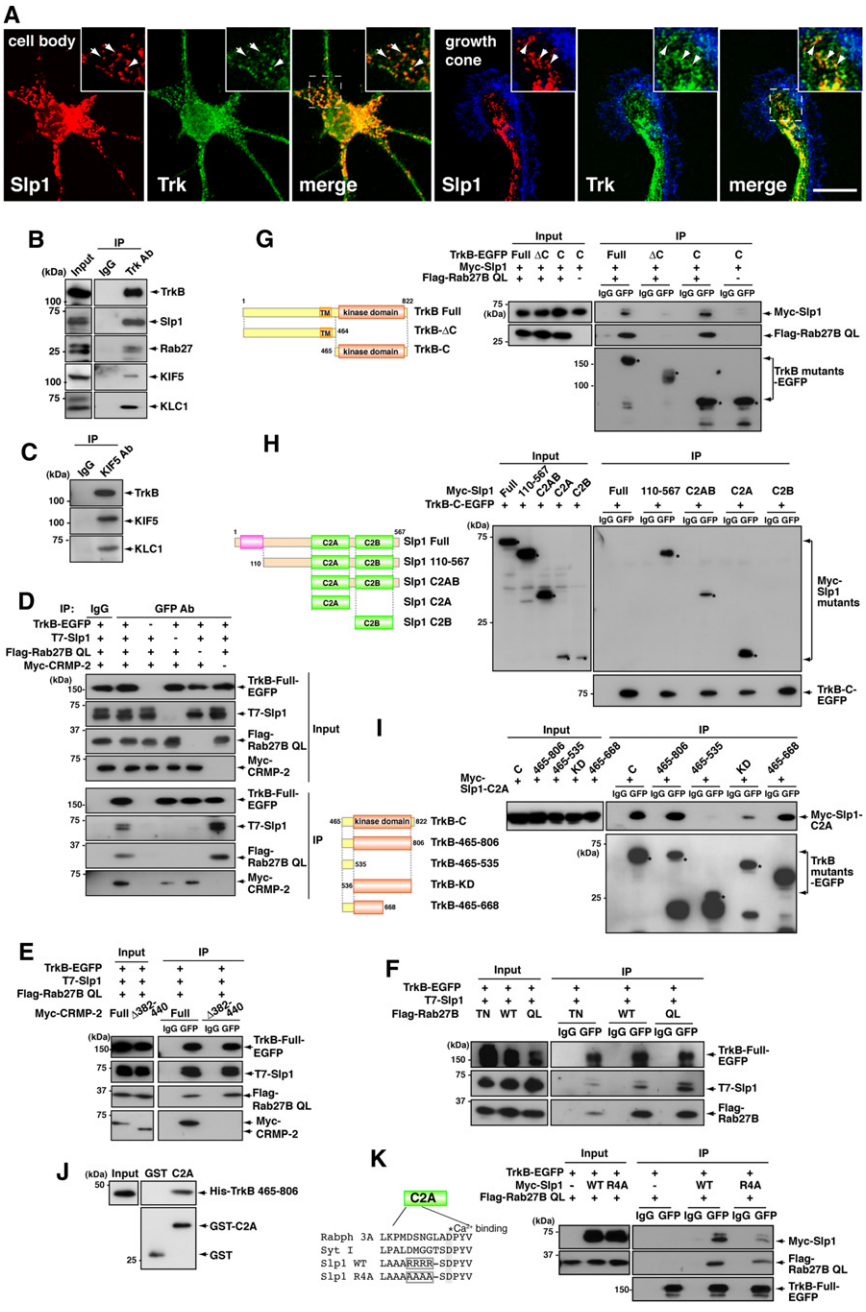

Figure 3. Association of the Slp1/Rab27B/CRMP-2 Complex with TrkB

(A) Colocalization of Slp1 and Trk at cell body and growth cone. Arrowheads in the enlarged images indicate colocalization of each protein.

(B and C) Complex formation of TrkB, Slp1, Rab27, and Kinesin-1 in vivo.

(D) The Slp1/Rab27B complex-dependent interaction with TrkB.

(E) The Slp1-binding domain (aa 382–440)-dependent interaction of CRMP-2 with TrkB.

(F) Activity-dependent association of Rab27B with Slp1 and TrkB.

(G) Mapping of the region in TrkB required for binding to Slp1/Rab27B.

(H) Mapping of the region in Slp1 required for binding to the TrkB cytoplasmic domain.

(I) Mapping of the region in TrkB required for binding to the Slp1 C2A domain.

(J) Direct interaction of the TrkB kinase domain with the Slp1 C2A domain in vitro.

(K) Effect of a point mutation in the Slp1 C2A domain on its association with TrkB.

in the absence of T7-Slp1 or Flag-Rab27B, but a CRMP-2 mutant lacking the Slp1-binding domain (Δ382–440) was not (Figure 3E). As His-CRMP-2 did not directly associate with GST-TrkB (Figure S1A), Myc-CRMP-2 may indirectly associate with TrkB-EGFP through the endogenous Slp1/Rab27B complex in COS-7 cells.

Next, we used immunoprecipitation analysis to examine whether this TrkB/Slp1/Rab27B association is dependent on the activity of Rab27B. When TrkB-EGFP was immunoprecipitated, Flag-Rab27B WT and Q78L were coimmunoprecipitated with T7-Slp1, whereas Flag-Rab27B T23N and coexpressed T7-Slp1 were weakly immunoprecipitated (Figure 3F). This suggests that Slp1 and Rab27B associate with TrkB in a manner dependent on the GTP-bound active form of Rab27B.

The Slp1 C2A Domain Associates with the Tyrosine Kinase Domain of TrkB

We then examined which region of TrkB binds to Slp1/Rab27B. The full-length and cytoplasmic region of TrkB (TrkB-C and aa 465–822) bound to the Myc-Slp1/Flag-Rab27B Q78L complex, whereas the cytoplasmic-deleted mutant (TrkB-ΔC) did not (Figure 3G). Myc-Slp1 did not associate with TrkB-C in the absence of Flag-Rab27B Q78L (Figure 3G), indicating that the TrkB cytoplasmic region associates with the Slp1/Rab27B complex. Which protein directly associates with TrkB? To answer this question, we used fragments of Slp1 for immunoprecipitation analysis. Interestingly, a Slp1 mutant lacking the Rab27-binding region (aa 110–567) bound to TrkB-C in the absence of Rab27B Q78L (Figure 3H). TrkB-C associated with the Slp1 C2AB and C2A domains, but not with the C2B domain (Figure 3H).

We also determined the C2A-binding region in TrkB. The Slp1 C2A domain associated with TrkB-C (aa 465–806 and aa 465–668) and associated weakly with the kinase domain (aa 536–806), but not with an aa 465–535 fragment (Figure 3I). The GST-C2A domain bound to His-TrkB in vitro (Figure 3J), suggesting that the C2A domain binds directly to the TrkB cytoplasmic region containing aa 465–668. To confirm that the C2A domain is responsible for the association of Slp1 with TrkB, we prepared a Slp1 mutant in which four arginine residues in aa 302–305

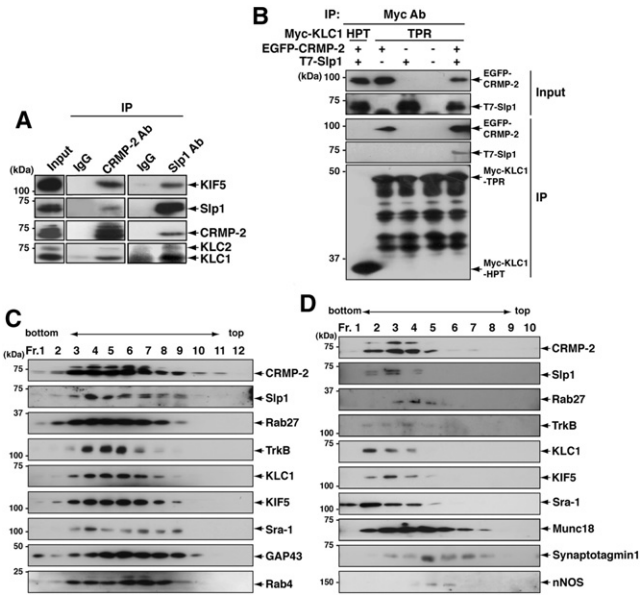

Figure 4. Slp1 Associates with Kinesin-1 via CRMP-2

(A) Complex formation of Slp1 and Kinesin-1 in vivo.

(B) The CRMP-2-dependent interaction between Slp1 and KLC1.

(C) The glycerol density gradient of growth cone vesicles (GCVs).

(D) The glycerol density gradient of detergent-extracted GCVs. The GCV fraction was extracted by using 2% Triton X-100, and then subjected to density gradient centrifugation.

(positively charged residues) were replaced by alanine residues (R4A mutant). The association of this mutant with TrkB was weaker than that of wild-type, suggesting that the C2A domain is important for the association with TrkB (Figure 3K).

Trk is known to be retrogradely transported with endosomal Rab proteins. Thus, we used immunoprecipitation analysis to examine whether endosomal Rabs (Rab4, Rab5, and Rab11) could be partners of Slp1/TrkB. When TrkB-EGFP was immunoprecipitated, constitutively active forms of Rab4A, Rab5A, and Rab11A were not coimmunoprecipitated with Slp1 (Figure S1E). We also found that active Rab3A and Rab6A were not coprecipitated by TrkB (data not shown). We could not obtain a clear result for Rab8 because it is expressed at too low a level in COS-7 cells (data not shown). We then examined the specificity of the transmembrane proteins including insulin-like growth factor-1 receptor β-subunit (IGF-1R), Neuropilin-1 (a receptor of Sema3A), and N-cadherin as partners of Slp1/Rab27B. Interestingly, the T7-Slp1/Flag-Rab27B Q78L complex was coimmunoprecipitated with IGF-1R, but not with Neuropilin-1 and N-cadherin (Figure S1F).

CRMP-2 Links Slp1 and TrkB to Kinesin-1

CRMP-2 interacts with the tetratricopeptide repeat domain of KLC1 and thereby links Kinesin-1 to tubulin dimers or Sra-1 as a cargo receptor (Kawano et al., 2005; Kimura et al., 2005). Thus, we next examined whether Slp1 associates with Kinesin-1 by immunoprecipitation analysis. We found that subunits of KIF5 and KLC1 were coimmunoprecipitated with Slp1 (Figure 4A). We then examined whether Slp1 could associate with Kinesin-1 through CRMP-2 in COS-7 cells. EGFP-CRMP-2 and T7-Slp1 were coimmunoprecipitated with the Myc-KLC1 tetratricopeptide repeat domain (aa 168–547, responsible for the cargo binding), but not with the Myc-KLC1 HPT domain (the heptad repeats domain, aa 1–167, responsible for KIF5 binding), whereas T7-Slp1 was not coimmunoprecipitated in the absence of CRMP-2 (Figure 4B), suggesting that Slp1 binds to KLC1 through CRMP-2.

We also examined whether Kinesin-1 forms a complex with TrkB. When TrkB was immunoprecipitated, KLC1 and KIF5 were coimmunoprecipitated together with Slp1, Rab27, and CRMP-2 (Figure 3B). When KIF5 was immunoprecipitated, TrkB and KLC1 were coimmunoprecipitated (Figure 3C).

To address whether Slp1, Rab27, CRMP-2, and Kinesin-1 are recruited on axonal vesicles that contain TrkB, we purified growth cone vesicles from embryonic rat brains and fractionated them with a 35%–70% glycerol gradient. The main populations of Slp1, Rab27, CRMP-2, Kinesin-1, and TrkB were present together in fractions 4, 5, and 6 (Fr. 4, 5, and 6) under conditions in which the peak fractions of Rab4 and GAP43 were Fr. 6, 7, and 8 (Figure 4C). This result supports the notion that Slp1/Rab27B/CRMP-2/Kinesin-1 associates with TrkB-containing vesicles. To characterize the TrkB complex, we extracted it from the growth cone vesicle fractions by using the detergent Triton X-100, and we performed 10%–35% glycerol density gradient centrifugation (Figure 4D). TrkB was fractionated in Fr. 2, 3, 4, and 5, and the S value was calculated to be ~11.3. CRMP-2 and KIF5 were present in Fr. 2, 3, 4, and 5; Slp1 was present in Fr. 2, 3, and 4; and Rab27 was present in Fr. 3, 4, and 5. Taken together, these results suggest that a subset of total cellular TrkB forms a complex with Slp1/Rab27/CRMP-2/Kinesin-1 under physiological conditions.

Slp1, CRMP-2, and Kinesin-1 Regulate Anterograde TrkB Transport

The existence of the TrkB/Slp1/Rab27B/CRMP-2/Kinesin-1 complex suggests that Slp1/Rab27B/CRMP-2 may mediate TrkB transport by Kinesin-1. To visualize TrkB transport in real time, we imaged live neurons expressing TrkB fused with mCherry (Shaner et al., 2004) by using time-lapse fluorescence microscopy. Vesicles containing TrkB-mCherry were observed particularly frequently in the perinuclear region, most likely in the Golgi apparatus (Figure 5A). Most vesicles were mobile and likely represented intracellular transport organelles moving anterogradely, retrogradely, and bidirectionally (Figure 5B; Movie S1). The greatest dynamic movement of TrkB-mCherry was observed in axons in developing hippocampal neurons (Figure 5C; Movie S1), so we then focused on the movements of TrkB-mCherry in axons. We categorized the pattern of vesicle movements during the period of image acquisition (0.3 s interval for 20 s) into four groups: (1) vesicles that moved only in the anterograde direction (anterograde), (2) vesicles that moved only in the retrograde direction (retrograde), (3) vesicles that moved in both directions (bidirectional), and (4) vesicles that were immobile (immobile). The retrograde transport vesicles were apparent more often than the anterograde vesicles and bidirectional vesicles (Figure 5D). The histogram of mean velocity revealed that both anterogradely and retrogradely transported TrkB-mCherry vesicles move at a broad range of average transport rates, ranging between 0.6 and 4.3 μm/s in axons (total

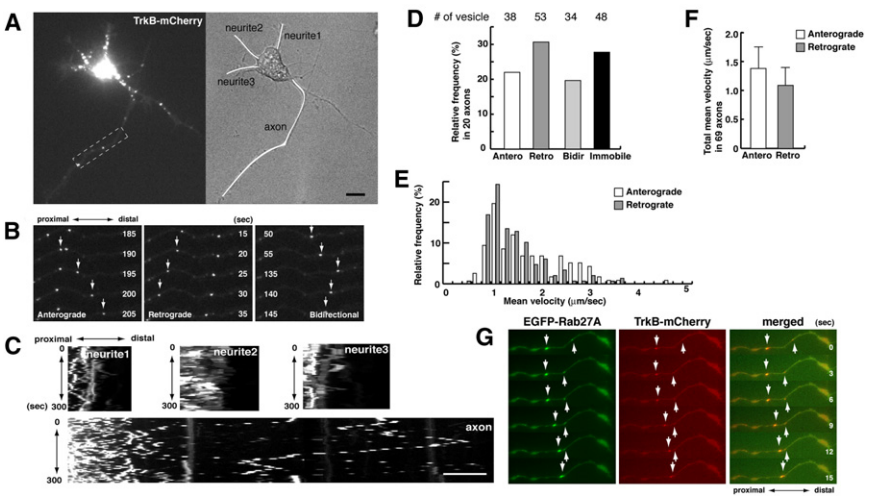

Figure 5. TrkB-mCherry Dynamically Moves in Axons

(A) Distribution of TrkB-mCherry in cultured rat hippocampal neurons. The white box indicates the area shown in (B). The white lines in the bright image on each neurite: immature neurites and the axon are indicated as "neurite1–3" and "axon," respectively, in (C). The scale bar represents 10 μm.

(B) Movement of TrkB-mCherry. White numbers indicate seconds. Arrows indicate the moving vesicles.

(C) Kymograph of each neurite indicated in (A). Images were captured every 5 s for 300 s in neurons.

(D–F) (D) Relative frequency of directional or bidirectional movements of TrkB-mCherry. Images were captured every 0.3 s for 20 s in every neuron, and the data were summarized as shown in panels (D)–(F). Anterograde (Antero), retrograde (Retro), bidirectional (Bidir), and immobile (Immobile) vesicles were classified as described in Results.

(E) The histogram depicts the relative frequency of the mean velocity distribution of anterograde or retrograde transport vesicles. (F) Total mean velocity of anterograde or retrograde transport of TrkB-mCherry vesicles in axons.

(G) Cotransport of TrkB-mCherry with EGFP-Rab27A. The vesicles of TrkB-mCherry and EGFP-Rab27A are indicated by arrows.

mean velocity, anterograde: 1.38 ± 0.4 μm/s; retrograde: 1.09 ± 0.34 μm/s; Figures 5E and 5F).

We next assessed whether Slp1, CRMP-2, and Kinesin-1 are involved in TrkB transport. We first tried to examine dual-color live cell imaging by using TrkB-mCherry and EGFP-fused Slp1, CRMP-2, or KLC1; however, all EGFP proteins were diffuse and were difficult to monitor on vesicular structures (data not shown), probably because a certain proportion of each protein dissociates from vesicles in an inactivate state and/or associates with cytosolic protein partners for other functions. Thus, we used EGFP-Rab27A, which has been reported to be clearly localized on vesicular structures in PC12 cells (Handley et al., 2007). Using this construct, we could confirm that EGFP-Rab27A was cotransported with TrkB-mCherry (Figure 5G).

For further examination of the functions of Slp1, CRMP-2, and KLC, we depleted each protein by small interfering RNA (siRNA) interference. The neurons were cotransfected with TrkB-mCherry and siRNA against Slp1, CRMP-2 (Nishimura et al., 2003), or KLC (Kimura et al., 2005) before plating. Next, we newly constructed siRNA against Slp1 and confirmed the effect of siRNA by immunoblot (Figure 6A) and immunostaining analyses (Figure 6B).

We then examined the motility of TrkB-mCherry in siRNA-transfected hippocampal neurons. Knockdown of Slp1, CRMP-2, or KLC decreased the number of TrkB-mCherry-positive vesicles in axons to ~two-thirds of the control number (Figure 6E). In particular, the vesicles categorized as anterograde were decreased in Slp1, CRMP-2, or KLC knockdown neurons, compared with control neurons (Figures 6C and 6E). To confirm these negative effects of protein depletion, we performed rescue experiments by using RNAi-resistant full-length Slp1 (rrSlp1), CRMP-2 (rrCRMP-2), and KLC1 (rrKLC1) (Figures 6D and 6E). The expression of RNAi-resistant mutants restored the expression levels of the respective proteins in siRNA-transfected cells (Figure 6D). The negative effect on the anterogradely transported TrkB-mCherry was rescued by the expression of Myc-rrSlp1 (Figure 6E). Similar results were obtained when we used rrCRMP-2 and rrKLC1 (Figure 6E). Because there is a possibility that the defect of axon structure caused by the knockdown of Slp1, CRMP-2, and KLC1 prevents TrkB movements, we observed the movement of Golgi vesicles stained by the fluorescence dye BODIPY-TR C5-ceramide. There was no clear difference between the movement of control and knockdown neurons (Figures S1G and S1H). We also confirmed that the localization of mitochondria is not affected by the siRNA treatment (Figure S1I). These results suggest that the decrease of anterograde movement of TrkB is not caused by a structural defect in neurite formation.

We then examined the motility of TrkB-mCherry in Rab27-depleted neurons. Knockdown of Rab27A/B was confirmed by immunoblot (Figure 6F) and immunostaining analyses (Figure 6G). We performed rescue experiments with RNAi-resistant full-length Rab27B (rrRab27B). The expression of a constitutively active form of rrRab27 restored the expression levels of Rab27 protein in siRNA-transfected cells (Figure 6H). Knockdown of Rab27 decreased the ratio of anterogradely transported TrkB-mCherry vesicles compared with control, and this negative effect was rescued by the expression of Myc-rrRab27B Q78L (Figure 6I). Consistent with these observations, expression of a constitutively active Rab27B mutant (Q78L) increased the rate of anterograde transport, whereas a dominant-negative mutant (T23N) did not exhibit this activity (Figure 6I).

We also examined the endogenous TrkB localization in Slp1, CRMP-2, or KLC1 knocked down neurons. The transfected neurons were detected by cotransfected EGFP (Figure 7A). Accumulation of endogenous TrkB at the distal part of the axon (30 μm from the tip of the axon) was significantly decreased by depletion of Slp1, CRMP-2, or KLC1 (Figures 7A and 7B). We also examined the effect of dominant-negative mutants of Slp1 (aa 1–109), Rab27B (T23N), CRMP-2 (ΔN440), and KIF5A (HL, lacking motor domain; aa 402–1028) (Kimura et al., 2005; Nakata and Hirokawa, 2003; Taya et al., 2007) on the localization of endogenous TrkB. A decrease in TrkB immunolabeling was observed at the distal part of axons in neurons expressing these dominant-negative mutants (Figures 7A and 7B). We found that the dominant-negative mutants generated more severe effects

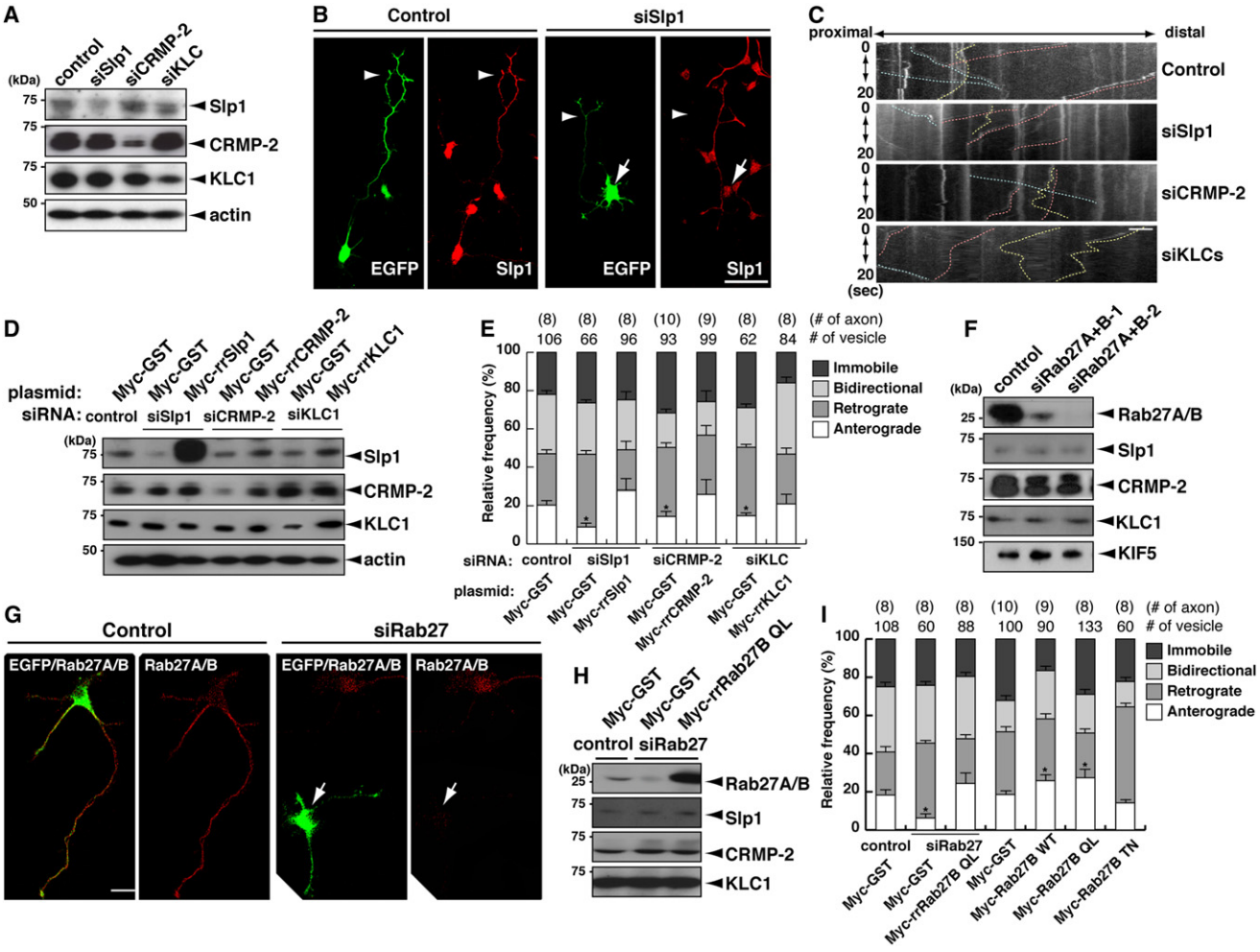

Figure 6. Depletion of Slp1, CRMP-2, KLC, and Rab27A/B Results in the Partial Inhibition of Anterograde TrkB Vesicle Transport

(A) Depletion of Slp1, CRMP-2, and KLC1 in hippocampal neurons by siRNA. Neurons were transfected with siRNA duplexes targeting Slp1 (siSlp1), CRMP-2 (siCRMP-2), KLC1 (siKLC1), or their control siRNA and were collected 72 hr after transfection.

(B) Confirmation of Slp1 depletion by immunostaining analysis. Arrows indicate transfected neurons, and arrowheads indicate the axons of the transfected neurons. The scale represents 30 μm.

(C) Kymograph of each neuron cotransfected with TrkB-mCherry and siSlp1, siCRMP-2, siKLC1, or control siRNA. Three-color dotted lines indicate examples of vesicles moving anterogradely (blue), retrogradely (pink), or bidirectionally (yellow). The scale represents 10 μm.

(D) Overexpression of RNAi-resistant Slp1 (rrSlp1), CRMP-2 (rrCRMP-2), and KLC1 (rrKLC1).

(E) Relative frequency of directional or bidirectional movements of TrkB-mCherry in siRNA- and RNAi-resistant construct-transfected neurons. The asterisk indicates a significant difference from the control as assessed by the Student's t test ($p < 0.05$). Numbers indicated on the top of the graph indicate the numbers of counted vesicles and axons.

(F) Depletion of Rab27A/B in hippocampal neurons by siRNA. Hereafter, we used both siRab27A and siRab27B-2 for the knockdown of Rab27A/B.

(G) Confirmation of Rab27A/B depletion by immunostaining analysis. Arrows indicate transfected neurons. The scale represents 10 μm.

(H) Rescue experiment with RNAi-resistant Rab27B (rrRab27B Q78L).

(I) Relative frequency of directional or bidirectional movements of TrkB-mCherry in siRab27- and RNAi-resistant Rab27B construct-transfected neurons. The asterisk indicates a significant difference from the control as assessed by the Student's t test ($p < 0.05$).

for the localization of endogenous TrkB than for siRNA (Figure 7B). This result might be due to the fact that siRNA could not completely deplete endogenous proteins, whereas the dominant-negative mutants interfered with the function of endogenous proteins.

We then examined the amount of TrkB on axon surfaces by surface labeling. Knockdown of Slp1, Rab27, CRMP-2, or KLC reduced TrkB surface labeling in the axonal shaft, but not in the cell body (Figures S1J and S1K). Taken together, these results indicate that Slp1, Rab27B, CRMP-2, and Kinesin-1 are involved in the anterograde transport of TrkB in axons (Figure 7E).

TrkB transmits BDNF signals for cell survival and neurite outgrowth via specific signaling molecules, including ERK1/2 (Segal, 2003); thus, Kinesin-1-dependent transport of TrkB to the axon terminus could play a role in this signaling function. To test this hypothesis, we examined the effects of knockdown of Slp1, Rab27, CRMP-2, and KLC on BDNF-induced activation of ERK1/2. When hippocampal neurons were stimulated with

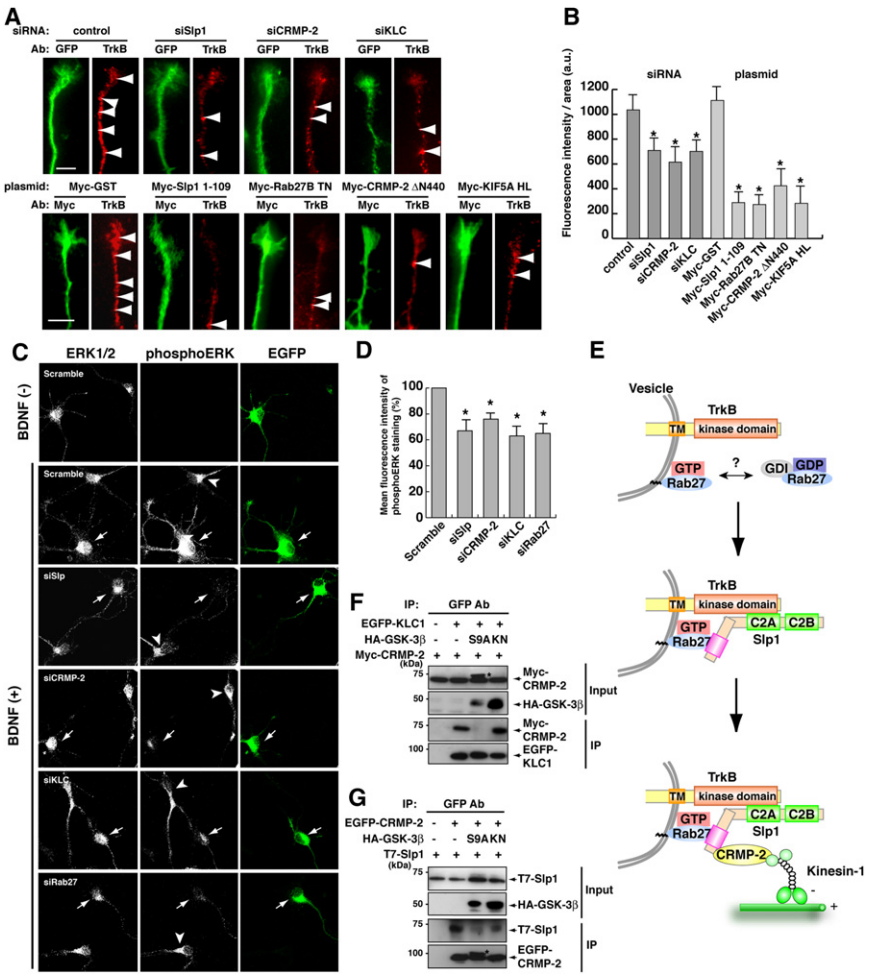

Figure 7. Depletion of Slp1, CRMP-2, KLC, and Rab27A/B Results in the Partial Disruption of TrkB Localization and BDNF-Induced ERK Phosphorylation

(A) Effect of depletion of Slp1, CRMP-2, and KLC1 and the overexpression of the dominant-negative form of Slp1, Rab27B, CRMP-2, and KIF5A on the localization of endogenous TrkB. The scale bar represents 10 μm.

(B) Quantitative analysis for the localization of endogenous TrkB at a distal axon in (A). The values shown are means ± standard errors of triplicate experiments. The asterisk indicates a significant difference from the control as assessed by the Student's t test ($p < 0.05$).

(C) BDNF-induced ERK1/2 phosphorylation in siRNA-transfected neurons. Arrows indicate the transfected neurons. Arrowheads indicate the untransfected neurons.

(D) Quantitative analysis of the mean fluorescence intensity of phosphorylation of ERK1/2 in siRNA-transfected neurons. The values shown are means ± standard errors of triplicate experiments. The asterisk indicates a significant difference from the control as assessed by the Student's t test ($p < 0.05$).

(E) Proposed model of TrkB transport. (1) Rab27 departs from GDI and recruited on TrkB-containing vesicles. (2) Slp1 binds to active Rab27 and TrkB on the vesicle surface. (3) The TrkB/Slp1/Rab27 complex associates with CRMP-2 and Kinesin-1 and is transported to the distal part of axons.

(F and G) Inhibition of the complex formation by phosphorylation induced by GSK-3β. A mobility shift of CRMP-2 (asterisk) was caused by phosphorylation at Thr-514 by GSK-3β.

BDNF, ERK1/2 phosphorylation was induced not only in the cell body, but also in the axonal shaft and terminus (Figure 7C). Knockdown of Slp1, Rab27B, CRMP-2, or KLC reduced immunolabeling of phosphorylated ERK1/2 elicited by BDNF stimulation in the axonal shaft and terminus, but not as much in the cell body (Figure 7D). This result supports the model that the recruitment of TrkB by Slp1/Rab27B/CRMP-2/Kinesin-1 to the axon terminus is critical for the proper signal transmission from BDNF.

We previously found that GSK-3β phosphorylates CRMP-2 and thereby disrupts the interaction of CRMP-2 with tubulin (Gartner et al., 2006; Jiang et al., 2005; Yoshimura et al., 2005). Thus, we hypothesized that GSK-3β might regulate the association of CRMP-2 with Slp1 and Kinesin-1. We found that transfection of constitutively active GSK-3β into COS-7 cells induced CRMP-2 phosphorylation and perturbed the association of CRMP-2 with Slp1 and KLC1 (Figures 7F and 7G). Thus, transport of TrkB might be regulated by kinases such as GSK-3β during neuronal polarization.

DISCUSSION

Rab GTPases have been implicated in the regulation of selective recognition in membrane trafficking (Pfeffer and Aivazian, 2004). However, it is still largely unclear how Rabs recognize specific vesicles for proper targeting. In this study, we found that Rab27 and its effector Slp1 recognize the cytoplasmic domain of the growth factor receptor TrkB through direct binding of Slp1 in a manner that is dependent on Rab27 activity. GTP-bound Rab27 appears to recognize the specific anterogradely transported vesicles containing Slp1 and TrkB (Figure 7E). Because a specific GDP dissociation inhibitor (GDI), a GDI displacement factor (GDF), and a guanine nucleotide exchange factor (GEF) for Rab27 have not yet been identified, it is unclear how Rab27 is activated and recruited to TrkB-containing vesicles. It is, however, important to remember that Rab27 is subjected to back extraction by GDI and GTPase activating protein (GAP). Given that, Slp1 association with Rab27 and TrkB may contribute to the localization of Rab27 on TrkB-containing vesicles, by limiting its diffusion in the membrane or by indirectly blocking Rab inactivation by a Rab GAP (Grosshans et al., 2006).

More importantly, this Rab recognition machinery is also recognized by the transport machinery, i.e., the cargo receptor CRMP-2 and the motor protein Kinesin-1. Kinesin-1 associates with TrkB through Rab27/Slp1 and CRMP-2 and anterogradely transports the TrkB-containing vesicles in developmental neurons. Interestingly, we found that the association of CRMP-2 with Slp1 or KLC1 is weakened by phosphorylation by GSK-3β. As the interaction between TrkB with Slp1 could be regulated

by Rab27 via cycling between its GTP- and GDP-bound forms, our results imply the multiple potential points for transport regulation. More intensive analysis is underway to elucidate the mechanisms that control the connection of TrkB to Kinesin-1 and the transport of TrkB.

We also found that other TrkB or Kinesin-1 adaptor proteins, such as ARMS/Kidins 220 (Bracale et al., 2007; Chang et al., 2004) and JIP2 (Verhey et al., 2001), are localized on TrkB vesicles at the growth cones. It is not surprising that a given vesicle has several different transmembrane and binding proteins, and that these proteins associate with a particular type of adaptor protein and/or motor protein. Since the reduction of TrkB targeting to the axonal surface and ERK1/2 phosphorylation by the knockdown of Slp1, Rab27B, CRMP-2, or KLC was not complete, it is possible that TrkB transport is regulated by several transport machineries that are mediated by different adaptor proteins and multifunctional motor proteins. Our present study indicates that TrkB directly associates with Slp1/Rab27/CRMP-2/Kinesin-1, and that the depletion of each component inhibits the anterograde transport of TrkB, suggesting that this protein complex is one of the principal transport machineries of TrkB-containing vesicles in developing neurons. Further analysis is required for the elucidation of how many different cargo receptors interact with multifunctional motor proteins on one vesicle surface.

In this study, we examined the specificity of Rabs, and we found that Rab27 is a specific Rab for Slp1 and TrkB association. As the functions of Rab27A and Rab27B seem redundant (Barral et al., 2002), it s not surprising that both Rab27A and Rab27B can associate with TrkB. Since Rab27B is more predominantly expressed than Rab27A in the brain, Rab27B seems to be the major physiological contributor. Although other Rabs (Rab3, Rab4, Rab5, Rab6, Rab8, and Rab11) were not coimmunoprecipitated with Slp1 and TrkB, Rab5 and Rab7 do appear to associate with retrogradely transported vesicles containing TrkB (Deinhardt et al., 2006). We also found that Rab8 was coimmunoprecipitated with TrkB from rat brain lysate. These results suggest that other Rabs may directly or indirectly associate with vesicles containing TrkB through their specific effectors and support the whole life cycle of TrkB-containing vesicles.

We previously reported that CRMP-2 plays a key role in axon specification and neuronal polarity (Inagaki et al., 2001; Yoshimura et al., 2005). CRMP-2 is dephosphorylated downstream of the BDNF/PI3-kinase/Akt/GSK-3β signaling cascade, and this dephosphorylated form of CRMP-2 enhances axon elongation (Gartner et al., 2006; Jiang et al., 2005; Yoshimura et al., 2005). Localized application of BDNF to the tip of an immature neurite consistently induces its axon differentiation and elongation (Shelly et al., 2007). These results suggest that in the distal part of neurites, TrkB has important roles in axon formation, acting through the PI3-kinase/Akt/GSK-3β pathway. In the present study, we found that depletion of CRMP-2 reduced the amount of TrkB in the axonal membrane and decreased the input signals (ERK1/2 phosphorylation) from BDNF stimulation, suggesting that CRMP-2 mediates BDNF signals via two distinct pathways: recruitment of TrkB into the distal part of an axon and enhancement of axon elongation through microtubule formation induced by dephosphorylation of CRMP-2. Interestingly, ARMS/Kidins220, which associates with TrkA and acts as a major mediator of prolonged ERK signaling induced by BDNF (Chang et al., 2004), is also detected on TrkB-containing vesicles. ARMS/Kidins220 also binds to KLC1 (Bracale et al., 2007). Therefore, our results raise the possibility that some mediators of BDNF signals might be simultaneously transported with TrkB to the distal part of axons, and that this might improve the efficiency of the BDNF-induced downstream signaling cascade.

EXPERIMENTAL PROCEDURES

Materials and Chemicals

Polyclonal anti-Slp1 antibody raised against the GST-Slp1 N-terminal domain (aa 1–109), polyclonal anti-CRMP-2 antibody, and polyclonal anti-Sra-1 antibody were produced as previously described (Arimura et al., 2000). This Slp1 antibody selectively recognizes Slp1, but not Slp2-a or Slp2-b (data not shown). The following antibodies were used: monoclonal anti-CRMP-2 and polyclonal anti-Rab27 antibodies (IBL, Gunma, Japan); polyclonal anti-GFP antiserum (Molecular Probes, Eugene, OR); monoclonal anti-GFP antibody (Roche, Indianapolis, IN); monoclonal anti-T7 antibody (Novagen, Darmstadt, Germany); monoclonal anti-Flag antibody (Sigma, St. Louis, MO); polyclonal anti-Myc and monoclonal anti-Trk antibodies (Santa Cruz Biotechnology, Santa Cruz, CA); monoclonal anti-TrkB, monoclonal Munc-18, monoclonal anti-synaptotagmin1, polyclonal anti-nNOS, monoclonal anti-Rab27, monoclonal Rab4, and monoclonal anti-ERK1/2 antibodies (BD Biosciences, Lexington, KY); monoclonal anti-KIF5, monoclonal anti-KLC, and monoclonal anti-GAP43 antibodies (Chemicon, Pittsburgh, PA); polyclonal anti-phosphoERK1/2 antibody (Cell Signaling, Inc., Danvers, MA); monoclonal anti-unique β-tubulin monoclonal antibody (TUJ1) (Berkeley Antibody Company, Berkeley, CA). BODIPY-TR C5-ceramide, Alexa 488-, Alexa 594-, and Alexa 647-conjugated secondary antibodies against mouse or rabbit immunoglobulin or phalloidin were purchased from Molecular Probes. BDNF was purchased from PeproTech EC, Ltd. (London, UK). Other materials and chemicals were obtained from commercial sources.

Plasmid Constructs and Protein Purification

The complementary DNAs (cDNAs) encoding CRMP-2 (Arimura et al., 2000), Slp1 (Fukuda and Mikoshiba, 2001), Slp2-b (Fukuda et al., 2001), KIF5 (Kimura et al., 2005), Rab27A, Rab27B (Imai et al., 2004), and TrkB (Watson et al., 1999) were obtained as described previously. The cDNA encoding mCherry was kindly provided by Dr. R.Y. Tsien (University of California, San Diego [UCSD]). pEGFP-Rab27A was kindly provided by Dr. R.D. Burgoyne (University of Liverpool, Liverpool, UK). The Slp1 point mutant was generated with a site-directed mutagenesis kit (Stratagen, La Jolla, CA).

SiRNA and siRNA-Resistant Slp1

The 21 oligonucleotide siRNA duplex was synthesized by Greiner Japan (Tokyo). The sequences of siRNAs against CRMP-2 (Nishimura et al., 2003), KLC1 (Kimura et al., 2005), or control siRNA (scramble) (Nishimura et al., 2003) were reported previously. The siRNA sequence of siSlp1 was 5′-GAAGAGCTCTAAGGGGGAC-3′ in rat Slp1 (GenBank accession number BC098679). The siRNA sequence of siRab27A was 5′-CCAGTGTACTGTACCAGTA-3′ in rat Rab27A. The siRNA sequence of siRab27B-1 was 5′-CAGAGTTTCTTGAATGTCA-3′ in rat Rab27B, and that of siRab27B-2 was 5′-CAACATTTCTTTACCGATA-3′ in rat Rab27B. Mouse Slp1 cDNA was used as RNA interference (RNAi)-resistant Slp1 (shown as rrSlp1), which does not include the rat Slp1 siRNA-targeted sequence in the corresponding sequence, 5′-GAAGAGCCCAAAGGGGGAC-3′ (the distinct nucleotides from rat Slp1 siRNA-targeting sequence are underlined). Mouse Rab27B cDNA was used as RNAi-resistant Rab27B (rrRab27B), which does not include the rat Rab27B siRNA-targeted sequence in the corresponding sequence, 5′-CAACATTTCTCTATAGATA-3′ (the distinct nucleotides from rat Rab27B siRNA-targeting sequence [siRab27B-2] are underlined). RNAi-resistant CRMP-2 (rrCRMP-2) was reported previously (Kawano et al., 2005). RNAi-resistant KLC1 (rrKLC1) was generated with a site-directed mutagenesis kit by using primer 5′-GAAGAAGTACGACGATGACATCTCCCCC-3′.

Other Experimental Procedures

Detailed protocols used in this study are described in Supplemental Data because of space limitations.

SUPPLEMENTAL DATA

Supplemental Data include one figure, one movie, and Supplemental Experimental Procedures and can be found with this article online at http://www.developmentalcell.com/supplemental/S1534-5807(09)00095-1.

ACKNOWLEDGMENTS

We thank R.Y. Tsien (UCSD); M. Igarashi (Niigata University); Y. Fukata (National Institute for Physiological Sciences); T. Suzuki (Hokkaido University); R.D. Burgoyne (University of Liverpool); M. Chao (New York University School of Medicine); and T. Watanabe, M. Takefuji, and N. Mishima (Nagoya University) for helpful discussions and preparation of some materials. We also thank T. Ishii for secretarial and technical assistance. This work was supported by Core Research for Evolutional Science and Technology (CREST) of the Japan Science and Technology Agency (JST); grant (S) 20227006 from grants-in-aid for scientific research (K.K.) from the Ministry of Education, Culture, Sports, Science and Technology of Japan (MEXT); grant 15GS0319 from grants-in-aid for creative scientific research from the Japan Society for the Promotion of Science (JSPS) (K.K.); grant 17024024 from grants-in-aid for scientific research on priority areas from MEXT (K.K.); a grant-in-aid for GCOE research from MEXT; grant 20-9883 from grants-in-aid for JSPS Fellows (S.N.); grants (B) 18700314 and 20700332 (N.A.) from grants-in-aid for young scientists from MEXT; and research grant 18-8 for Nervous and Mental Disorders from the Ministry of Health, Labour and Welfare.

Received: July 9, 2008
Revised: November 25, 2008
Accepted: March 3, 2009
Published: May 18, 2009

REFERENCES

Arimura, N., and Kaibuchi, K. (2007). Neuronal polarity: from extracellular signals to intracellular mechanisms. Nat. Rev. Neurosci. *8*, 194–205.

Arimura, N., Inagaki, N., Chihara, K., Menager, C., Nakamura, N., Amano, M., Iwamatsu, A., Goshima, Y., and Kaibuchi, K. (2000). Phosphorylation of collapsin response mediator protein-2 by Rho-kinase. Evidence for two separate signaling pathways for growth cone collapse. J. Biol. Chem. *275*, 23973–23980.

Barral, D.C., Ramalho, J.S., Anders, R., Hume, A.N., Knapton, H.J., Tolmachova, T., Collinson, L.M., Goulding, D., Authi, K.S., and Seabra, M.C. (2002). Functional redundancy of Rab27 proteins and the pathogenesis of Griscelli syndrome. J. Clin. Invest. *110*, 247–257.

Bracale, A., Cesca, F., Neubrand, V.E., Newsome, T.P., Way, M., and Schiavo, G. (2007). Kidins220/ARMS is transported by a kinesin-1-based mechanism likely to be involved in neuronal differentiation. Mol. Biol. Cell *18*, 142–152.

Chang, M.S., Arevalo, J.C., and Chao, M.V. (2004). Ternary complex with Trk, p75, and an ankyrin-rich membrane spanning protein. J. Neurosci. Res. *78*, 186–192.

Da Silva, J.S., Hasegawa, T., Miyagi, T., Dotti, C.G., and Abad-Rodriguez, J. (2005). Asymmetric membrane ganglioside sialidase activity specifies axonal fate. Nat. Neurosci. *8*, 606–615.

Deinhardt, K., Salinas, S., Verastegui, C., Watson, R., Worth, D., Hanrahan, S., Bucci, C., and Schiavo, G. (2006). Rab5 and Rab7 control endocytic sorting along the axonal retrograde transport pathway. Neuron *52*, 293–305.

Fukata, Y., Itoh, T.J., Kimura, T., Menager, C., Nishimura, T., Shiromizu, T., Watanabe, H., Inagaki, N., Iwamatsu, A., Hotani, H., et al. (2002). CRMP-2 binds to tubulin heterodimers to promote microtubule assembly. Nat. Cell Biol. *4*, 583–591.

Fukuda, M. (2002). Synaptotagmin-like protein (Slp) homology domain 1 of Slac2-a/melanophilin is a critical determinant of GTP-dependent specific binding to Rab27A. J. Biol. Chem. *277*, 40118–40124.

Fukuda, M., and Mikoshiba, K. (2001). Synaptotagmin-like protein 1-3: a novel family of C-terminal-type tandem C2 proteins. Biochem. Biophys. Res. Commun. *281*, 1226–1233.

Fukuda, M., Saegusa, C., and Mikoshiba, K. (2001). Novel splicing isoforms of synaptotagmin-like proteins 2 and 3: identification of the Slp homology domain. Biochem. Biophys. Res. Commun. *283*, 513–519.

Gartner, A., Huang, X., and Hall, A. (2006). Neuronal polarity is regulated by glycogen synthase kinase-3 (GSK-3β) independently of Akt/PKB serine phosphorylation. J. Cell Sci. *119*, 3927–3934.

Glebova, N.O., and Ginty, D.D. (2005). Growth and survival signals controlling sympathetic nervous system development. Annu. Rev. Neurosci. *28*, 191–222.

Goldstein, L.S. (2001). Molecular motors: from one motor many tails to one motor many tales. Trends Cell Biol. *11*, 477–482.

Gomes, R.A., Hampton, C., El-Sabeawy, F., Sabo, S.L., and McAllister, A.K. (2006). The dynamic distribution of TrkB receptors before, during, and after synapse formation between cortical neurons. J. Neurosci. *26*, 11487–11500.

Grosshans, B.L., Ortiz, D., and Novick, P. (2006). Rabs and their effectors: achieving specificity in membrane traffic. Proc. Natl. Acad. Sci. USA *103*, 11821–11827.

Handley, M.T., Haynes, L.P., and Burgoyne, R.D. (2007). Differential dynamics of Rab3A and Rab27A on secretory granules. J. Cell Sci. *120*, 973–984.

Hirokawa, N., and Takemura, R. (2005). Molecular motors and mechanisms of directional transport in neurons. Nat. Rev. Neurosci. *6*, 201–214.

Imai, A., Yoshie, S., Nashida, T., Shimomura, H., and Fukuda, M. (2004). The small GTPase Rab27B regulates amylase release from rat parotid acinar cells. J. Cell Sci. *117*, 1945–1953.

Inagaki, N., Chihara, K., Arimura, N., Menager, C., Kawano, Y., Matsuo, N., Nishimura, T., Amano, M., and Kaibuchi, K. (2001). CRMP-2 induces axons in cultured hippocampal neurons. Nat. Neurosci. *4*, 781–782.

Izumi, T., Gomi, H., Kasai, K., Mizutani, S., and Torii, S. (2003). The roles of Rab27 and its effectors in the regulated secretory pathways. Cell Struct. Funct. *28*, 465–474.

Jiang, H., Guo, W., Liang, X., and Rao, Y. (2005). Both the establishment and the maintenance of neuronal polarity require active mechanisms: critical roles of GSK-3β and its upstream regulators. Cell *120*, 123–135.

Kawano, Y., Yoshimura, T., Tsuboi, D., Kawabata, S., Kaneko-Kawano, T., Shirataki, H., Takenawa, T., and Kaibuchi, K. (2005). CRMP-2 is involved in Kinesin-1-dependent transport of the Sra-1/WAVE1 complex and axon formation. Mol. Cell. Biol. *25*, 9920–9935.

Kim, W.Y., Zhou, F.Q., Zhou, J., Yokota, Y., Wang, Y.M., Yoshimura, T., Kaibuchi, K., Woodgett, J.R., Anton, E.S., and Snider, W.D. (2006). Essential roles for GSK-3s and GSK-3-primed substrates in neurotrophin-induced and hippocampal axon growth. Neuron *52*, 981–996.

Kimura, T., Arimura, N., Fukata, Y., Watanabe, H., Iwamatsu, A., and Kaibuchi, K. (2005). Tubulin and CRMP-2 complex is transported via Kinesin-1. J. Neurochem. *93*, 1371–1382.

Kuroda, T.S., Fukuda, M., Ariga, H., and Mikoshiba, K. (2002). The Slp homology domain of synaptotagmin-like proteins 1-4 and Slac2 functions as a novel Rab27A binding domain. J. Biol. Chem. *277*, 9212–9218.

Nakata, T., and Hirokawa, N. (2003). Microtubules provide directional cues for polarized axonal transport through interaction with kinesin motor head. J. Cell Biol. *162*, 1045–1055.

Nishimura, T., Fukata, Y., Kato, K., Yamaguchi, T., Matsuura, Y., Kamiguchi, H., and Kaibuchi, K. (2003). CRMP-2 regulates polarized Numb-mediated endocytosis for axon growth. Nat. Cell Biol. *5*, 819–826.

Pfeffer, S., and Aivazian, D. (2004). Targeting Rab GTPases to distinct membrane compartments. Nat. Rev. Mol. Cell Biol. *5*, 886–896.

Segal, R.A. (2003). Selectivity in neurotrophin signaling: theme and variations. Annu. Rev. Neurosci. *26*, 299–330.

Shaner, N.C., Campbell, R.E., Steinbach, P.A., Giepmans, B.N., Palmer, A.E., and Tsien, R.Y. (2004). Improved monomeric red, orange and yellow fluorescent proteins derived from *Discosoma* sp. red fluorescent protein. Nat. Biotechnol. *22*, 1567–1572.

Shelly, M., Cancedda, L., Heilshorn, S., Sumbre, G., and Poo, M.M. (2007). LKB1/STRAD promotes axon initiation during neuronal polarization. Cell *129*, 565–577.

Strom, M., Hume, A.N., Tarafder, A.K., Barkagianni, E., and Seabra, M.C. (2002). A family of Rab27-binding proteins. Melanophilin links Rab27a and myosin Va function in melanosome transport. J. Biol. Chem. *277*, 25423–25430.

Takamori, S., Holt, M., Stenius, K., Lemke, E.A., Gronborg, M., Riedel, D., Urlaub, H., Schenck, S., Brugger, B., Ringler, P., et al. (2006). Molecular anatomy of a trafficking organelle. Cell *127*, 831–846.

Taya, S., Shinoda, T., Tsuboi, D., Asaki, J., Nagai, K., Hikita, T., Kuroda, S., Kuroda, K., Shimizu, M., Hirotsune, S., et al. (2007). Dros. Inf. Serv.C1 regulates the transport of the NUDEL/LIS1/14-3-3epsilon complex through kinesin-1. J. Neurosci. *27*, 15–26.

Tsuboi, D., Hikita, T., Qadota, H., Amano, M., and Kaibuchi, K. (2005). Regulatory machinery of UNC-33 Ce-CRMP localization in neurites during neuronal development in *Caenorhabditis elegans*. J. Neurochem. *95*, 1629–1641.

Verhey, K.J., Meyer, D., Deehan, R., Blenis, J., Schnapp, B.J., Rapoport, T.A., and Margolis, B. (2001). Cargo of kinesin identified as JIP scaffolding proteins and associated signaling molecules. J. Cell Biol. *152*, 959–970.

Watson, F.L., Heerssen, H.M., Moheban, D.B., Lin, M.Z., Sauvageot, C.M., Bhattacharyya, A., Pomeroy, S.L., and Segal, R.A. (1999). Rapid nuclear responses to target-derived neurotrophins require retrograde transport of ligand-receptor complex. J. Neurosci. *19*, 7889–7900.

Yoshimura, T., Kawano, Y., Arimura, N., Kawabata, S., Kikuchi, A., and Kaibuchi, K. (2005). GSK-3β regulates phosphorylation of CRMP-2 and neuronal polarity. Cell *120*, 137–149.

Zhao, S., Torii, S., Yokota-Hashimoto, H., Takeuchi, T., and Izumi, T. (2002). Involvement of Rab27b in the regulated secretion of pituitary hormones. Endocrinology *143*, 1817–1824.

Zhou, F.Q., and Snider, W.D. (2005). Cell biology. GSK-3β and microtubule assembly in axons. Science *308*, 211–214.